

A natom y of a gauge theory

D irk K reim er

IHES, 35 rte. de Chartres, 91440 Bures-sur-Y vette, France

M arch 27, 2022

A bstract

W e exhibit the role of Hochschild cohomology in quantum eld theory with particular emphasis on gauge theory and Dyson-Schwinger equations, the quantum equations of motion. These equations emerge from Hopf- and Lie algebra theory and free quantum eld theory only. In the course of our analysis we exhibit an intimate relation between the Slavnov-Taylor identities for the couplings and the existence of Hopf sub-algebras defined on the sum of all graphs at a given loop order, surpassing the need to work on single diagrams.

0 Introduction

Over the last seven years many properties of the Hopf algebra structure of renormalization have been investigated, mostly on the mathematical side, with at least one notable exception [1] which showed how to solve a non-linear Dyson-Schwinger equation exactly, as opposed to a mere perturbation expansion.

In this paper, we explore the elementary relations between a perturbative expansion in quantum eld theory, the corresponding Hochschild cohomology and the equations of motion in the context of a generic gauge theory. A major feature underlying our analysis is the emphasis on free quantum eld theory and locality expressed through Hochschild cohomology. Together they specify the interacting theory. The novel phenomenon we report here is the interplay between the existence of a suitable sub Hopf algebra of perturbation theory and the existence of internal symmetries: the Slavnov-Taylor identities which ensure equality of renormalized couplings are equivalent to the existence of forest formulas indexed just by the loop number, the grading of the usual Hopf algebra of Feynman graphs.

0.1 The structure of Dyson-Schwinger equations

If one ultimately wants to address non-perturbative quantum eld theory one has to solve the corresponding Dyson-Schwinger equations exactly. This looks prohibitively difficult. But the recent progress with perturbative quantum eld theory also points towards methods of solutions for Dyson-Schwinger equations [1, 1]. Let us review the current situation. Detailed references can be found in [13].

Feynman graphs possess a Lie algebra structure which dually governs the structure of renormalization, via the forest formula. The corresponding Hopf algebra furnishes one-cocycles which ensure locality of counterterms. These one-cocycles allow to generate the

CNRS, also supported in parts by NSF grant DMS-0401262 at Center for Mathematical Physics, Boston University. Email: kreimer@ihes.fr

one-particle irreducible Green functions and provide the skeletons underlying the perturbative expansion. The one-cocycles correspond to primitive elements in the linear span of generators of the Hopf algebra and are graded by the loop number. One gets a set of embedded Hopf algebras from a hierarchy of Dyson-Schwinger equations based on primitive graphs up to n loops. Underlying this structure is a universal Hopf algebra structure whose generators are given by the sum of all graphs with a given loop number. Let us call this sub Hopf algebra the grading algebra [11, 3]. It is the existence of this grading algebra which allows for the recursions which made the non-perturbative methods of [1] feasible.

The purpose of the present paper is to exhibit this structure for the example of a non-abelian gauge theory. In particular, we exhibit the grading algebra of this theory and show that its existence is equivalent to the existence of the Slavnov-Taylor identities for the couplings.

Dyson-Schwinger equations, illuminating recursive structure in Green functions, are recently on the forefront again in different areas of field theory [14, 15, 16]. We expect that our results are a starting point to understand these phenomena more systematically. In particular, the representations of the rescaling group and hence the role of dilatations in quantum field theory is intimately connected to the role of the Hochschild one-cocycles above, and motivates our quest for understanding their role in non-perturbative quantum field theory.

0.2 Interaction vertices from free quantum fields and locality

We start with a free quantum field theory with free propagators given by the usual requirements of free field theory for fermion and boson fields.

Before we discuss how locality determines the structure of the full Green functions we look at the tree level first, for motivation. We want to emphasize in our approach the known fact that the Feynman rules for tree-level graphs are determined by free quantum field theory (which gives Feynman rules for the edges) and locality (which implies Feynman rules for the vertices).

So let us first remind ourselves how the quest for locality determines the interaction vertices in the context of renormalizable theories, without reference to a classical Lagrangian at this stage.

We exhibit the argument for the example of the QED vertex. Thus we aim to infer the local interaction vertex $v(q;p)$ for the interaction of a photon, with four-momentum $p = q$, with an e^+e^- pair, with four-momenta p and q .

We will infer the Feynman rule for the vertex from the knowledge of the free photon, electron and positron propagator, and from the requirement that we should be able to renormalize by local counterterms.

We start with an Ansatz that at tree-level the sought-after vertex must be of the form

$$v(q;p) = \sum_{i=1}^X a_i f^{[i]} = a_1 + a_2 \frac{pq}{q^2} + \dots; \quad (1)$$

in accordance with Lorentz covariance, spin representations and dimensions of the free propagators involved. Note that we can assume the coefficients a_i above to be constants: below we are only interested in the behaviour at large momentum transfer at each internal vertex. In that limit, each ratio in

$$u = \frac{q^2}{q^2 + p^2 + (p+q)^2}; v = \frac{p^2}{q^2 + p^2 + (p+q)^2}; w = \frac{(p+q)^2}{q^2 + p^2 + (p+q)^2} \quad (2)$$

turns to zero or one, so that $a_i(u;v;w)$ turns to a constant indeed.

We can now determine $v(q;p)$ as follows.

First, we note that free quantum field theory and the requirement for renormalizability provide us with powercounting. We hence construct the 1PI graph with lowest non-vanishing loop order corresponding to our interaction:



This graph is log-divergent. If we demand to have a renormalizable theory, its coefficient of log-divergence must be proportional to the sought after tree-level vertex. This is indeed the well-known clue. By construction, the graph has no subdivergences and hence will evaluate to an expression of the form

$$\text{Diagram} = v(q;p) \ln + \text{finite terms}; \quad (3)$$

where we cut-off momentum integrals by Λ . The important point is that the only part of this vertex functions which is allowed to diverge with Λ is the part proportional to the sought-after tree-level vertex, if we are in a renormalizable theory.

Hence, we can write

$$v(q;p) = \lim_{\Lambda \rightarrow \infty} \frac{1}{\Lambda^{Z_v+1}} \int d^4k \, v(q;k) \frac{1}{k^2 + m^2} v(k+q; k+p) \frac{1}{k^2 + m^2} v(k;p) D(k); \quad (4)$$

Inserting (1) we indeed find that

$$v(q;p) = \text{Diagram}; \quad (5)$$

as was to be expected.

Note that this states the obvious: in a local renormalizable quantum field theory the short-distance singularities can be absorbed by suitable modifications of parameters in the given Lagrangian. Vice-versa, if we make locality the starting point and hence require that short-distance singularities are self-similar to the tree-level terms, we obtain the interaction part of the Lagrangian from this requirement.

There is a cute albeit obvious message hidden here: if we settle on a given set of free fields and demand that they interact in a renormalizable manner, already the lowest loop order scattering processes fix the form of the interaction vertices from the knowledge of free quantum field theory and the requirement of locality, whilst the interaction part of the Lagrangian appears as a derived quantity. In this spirit we will continue to explore what we can learn about QFT, in particular about a gauge theory, starting from free covariances and so-determined interaction terms, and the accompanying one-particle irreducible graphs which go with them. Our guiding principle will still be locality, in its mathematical disguise as Hochschild cohomology.

In particular, we are now interested in formal sums of graphs corresponding to a specific instance of propagation or interaction: the sum of all 1PI graphs which constitute in perturbative QFT the 1PI Green function for that amplitude. The sum over all such 1PI Green functions furnishes then the effective action, by definition. We will study these 1PI Green functions for a non-abelian gauge theory.

We hence wish to discuss the formal sums

$$\Gamma^r = \sum_{j=0}^{\infty} g^{2j} \frac{1}{\text{sym}(j)}; \quad (6)$$

Here and in the following the superscript r specifies the Green function under consideration, it can be regarded as a collective label for the quantum numbers at the external legs of that function.

Already at this level interesting structure emerges. Our main tool will be the exploration of the Hochschild cohomology of the Hopf algebra structure which comes with such graphs. This Hochschild cohomology provides a mathematically precise formulation of locality [7, 4, 3], and will carry us far in the understanding of the structure of the theory.

0.3 Quantum equations of motion from Hochschild Cohomology

Such Hopf algebras have marvelous properties which they inherit from the universal object H_{rt} for such algebras: the commutative Hopf algebra of non-planar rooted trees [2].

In that context, it is beneficial to study Dyson-Schwinger equations as formal constructions based on the Hochschild cohomology of such Hopf algebras. Before we justify the connection to Dyson-Schwinger equation through the study of a generic gauge theory below, let us first describe the universal set-up on rooted trees [3].

First, we settle on say a suitable Hopf algebra A which can be H_{rt} or any suitable sub-Hopf algebra A .

Let A then be any such connected graded Hopf algebra which is free or free commutative as an algebra, and $(B_+^{d_n})_{n \geq 0}$ a collection of Hochschild 1-cocycles on it. The Dyson-Schwinger equation is

$$X = I + \sum_{n=1}^{\infty} w_n B_+^{d_n}(X^{n+1}) \quad (7)$$

in $A[[\hbar]]$: The parameter \hbar plays the role of a coupling constant. The w_n are scalars in k : We decompose the solution

$$X = \sum_{n=0}^{\infty} \hbar^n c_n \quad (8)$$

with $c_n \in A$:

Lemma 1 The Dyson-Schwinger equation (7) has a unique solution described by $c_0 = I$ and

$$c_n = \sum_{m=1}^{\infty} \hbar^m B_+^{d_m} \left(\sum_{k_1 + \dots + k_{m+1} = n-m; k_i \geq 0} c_{k_1} \dots c_{k_{m+1}} \right) \quad (9)$$

The c_n , coefficients in the n -th term of the perturbative expansion have a very nice property which we will rediscover in quantum field theory:

Theorem 2 The c_n generate a Hopf subalgebra (henceforth called the grading algebra) of A :

$$(c_n) = \sum_{k=0}^{\infty} \hbar^k P_{n,k} c_k \quad (10)$$

where the $P_{n,k}$ are homogeneous polynomials of degree $n-k$ in the c_i ; $1 \leq n$:

$$P_{n,k} = \sum_{l_1 + \dots + l_{k+1} = n-k} c_{l_1} \dots c_{l_{k+1}} \quad (11)$$

In particular, the $P_{n,k}$ are independent of the w_n and $B_+^{d_n}$:

In this paper we want to discuss this structure when we pass from the universal object H_{rt} to the concrete Hopf algebra of say a generic gauge theory. We aim at insights into the non-perturbative structure of QFT and also prepare for new methods of computation in subsequent work. In particular we use the fact that the operadic proof of the above theorem given in [3] extends to our case once the proper insertion maps for graph insertions have been defined. To see the main point, we study first an elementary example.

0.4 A toy Ward identity

Consider the following system of DSEs based on say four Hochschild one-cocycles.

$$X_1 = 1 + B_+^a(X_3 X_1) + B_+^b(X_2^2) \quad (12)$$

$$X_2 = 1 + B_+^c(X_2^2) \quad (13)$$

$$X_3 = 1 + B_+^d(X_3^2): \quad (14)$$

One immediately confirms that imposing the symmetry

$$X_1 X_3 = X_2^2 \quad (15)$$

in the Hopf algebra is equivalent to giving the sub Hopf algebra, i2 f1;2;3g,

$$X_i = 1 + \sum_n X_n C_n^{(i)} \quad (16)$$

$$(C_n^{(i)}) = \sum_{k=0}^n P_{n,k}^{(i)} C_{n-k}^{(i)}; \quad (17)$$

where the polynomials $P_{njk}^{(2)}$ and $P_{njk}^{(3)}$ are easily determined as in (10). Similarly, upon using the symmetry (15) we find a new equation for X_1

$$X_1 = 1 + \overset{h}{B_+^a} + \overset{i}{B_+^b} (X_1 X_c); \quad (18)$$

where $X_c = X_3 = X_2^2 = X_1$, and all elements $c_n^{(1)}$ are symmetric in exchange of labels a and b . The existence of a sub Hopf algebra on the generators $c_n^{(i)}$ is now straightforward to establish as in [3].

We will now focus on the case of a generic non-abelian gauge theory, and exhibit how the Hochschild cohomology of the Hopf algebra of its perturbative expansion, the equations of motion and local gauge symmetry interfere. In particular, we will find a similar situation: the existence of a sub Hopf algebra is equivalent to the existence of relations exhibiting symmetries between Green functions.

To formulate our results we first introduce the pre-Lie algebra of Feynman graphs in this context in the next section.

We then introduce our result and discuss it with the help of a completely worked out two-loop example.

1 Graphs

In this section we first define graphs and the accompanying pre-Lie and Hopf algebras. The material is a straightforward application of previous results to a generic gauge theory.

1.1 The set of graphs

All graphs we consider are built from the following set R of edges and vertices

$$R = \overset{n}{\longrightarrow} + \text{---} + \text{---} + \text{---} + \text{---} + \text{---} + \text{---} + \dots \quad (19)$$

We subdivide into edges and vertices,

[illegible]

and

$$R_E = \text{---} ; \text{---} ; \text{---} g : \quad (21)$$

Obviously, $R = R_E \cup R_V$. We have included edges for the free propagation of the local gauge field, corresponding ghost fields, and fermion fields as the only matter fields. We exclude the discussion of scalar matter fields coupled to gauge fields which deserve a separate discussion in future work. We thus include only the expected vertices in a generic local gauge theory: triple and quartic self-interactions of the gauge field, an interaction of the gauge field with its ghost field and minimal interaction between the gauge and matter fields - R_V is determined by R_E and locality in the spirit of the argument in the previous section.

We then define one-particle irreducible (1PI) graphs as usual: they remain connected after removal of any one of the internal edges. For such a 1PI graph we have external legs $^{[1]}_{\text{ext}}$, internal edges $^{[1]}_{\text{int}}$ and vertices $^{[0]}$.

For any 1PI graph we let $\text{res}(\cdot)$ be the graph when all its internal edges shrink to a point

$$\text{res}(\text{---}) = \text{---} : \quad (22)$$

We call $\text{res}(\cdot)$ the residue of to emphasize that a graph provides a counterterm $S_R(\cdot)$ which contributes $S_R(\cdot) - \text{res}(\cdot)$ to the Lagrangian

$$L = \sum_{r \in R_E} 1 = (r) + \sum_{r \in R_V} (r); \quad (23)$$

where we note that for $r \in R_E$ we have $1 = (r)$ as the inverse free propagator, as it should be. We extend the notion of a residue of a graph to a product $\cdot_i(\cdot_i)$ of graphs:

$$\text{res}(\cdot_i \cdot_i) = \cdot_i \text{res}(\cdot_i); \quad (24)$$

Any element r in R has a superficial degree of divergence $\text{sdd}(r)$, given as follows

$$\begin{aligned} w(\text{---}) &= 1; w(\text{---}) = 1; w(\text{---}) = 2; w(\text{---}) = 0; \\ w(\text{---}) &= 0; w(\text{---}) = -1; w(\text{---}) = 0; \end{aligned} \quad (25)$$

We introduce the loop number j

$$j = \text{rank}(H_1(\cdot)); \quad (26)$$

where $H_1(\cdot)$ is the first homology group of \cdot , and

$$\sum_i Y_i = \sum_i X_i j_i; \quad (27)$$

For a 1PI graph we let then its superficial degree of divergence $w(\cdot)$ be

$$w(\cdot) = 4j + \sum_{p \in \text{p2}^{[1]}_{\text{int}}[^{[0]}]} w(p); \quad (28)$$

Note that all 1PI graphs which have $\text{sdd} \leq 0$ have residue in the above finite set R - we are dealing with a renormalizable theory. Here we are mainly interested in the structure of superficially divergent graphs, and hence do not discuss graphs and Green functions which are superficially convergent. For all $r \in R$, we let M_r be the set of graphs such that $\text{res}(\cdot) = r$.

1.2 Isotopy classes of graphs

The symmetry factor of a graph Γ , $\text{sym}(\Gamma)$, is defined as usual as the rank of the automorphism group of Γ .

We consider graphs up to the usual isotopy, for fixed external legs:

$$\text{Diagram 1} = \text{Diagram 2} \quad \text{Diagram 3} = \text{Diagram 4} : \quad (29)$$

This plays a role in the study of the pre-Lie structure on graphs below. Indeed, we note that the symmetry factor of a sum of all graphs belonging to an isotopy class is the product of the symmetry factor of the subgraphs times the symmetry factor of the cograph obtained by shrinking the subgraphs. This ensures compatibility of symmetry factors under graph insertions as in the following example.

$$\text{sym}(\text{Diagram 1} + \text{Diagram 2}) = 4 = \text{sym}(\text{Diagram 3}) \cdot \text{sym}(\text{Diagram 4}) ; \quad (30)$$

so that

$$\frac{1}{4} (\text{Diagram 1} + \text{Diagram 2}) = \frac{1}{\text{sym}(\text{Diagram 3})} \text{Diagram 4} ; \quad (31)$$

with

$$\text{sym}(\text{Diagram 1}) = \text{sym}(\text{Diagram 2}) = 2 : \quad (32)$$

1.3 Combinatorial Green functions

We can now speak of the set of supercially divergent 1PI graphs and consider graphs according to their residue and loop number j .

We define the formal sums

$$\chi_r = 1 + \sum_{2M_r} g^{2j} \frac{j}{\text{sym}(\Gamma)} ; r \in R_V ; \quad (33)$$

$$\chi_r = 1 + \sum_{2M_r} g^{2j} \frac{j}{\text{sym}(\Gamma)} ; r \in R_E : \quad (34)$$

We let

$$c_k^r = \sum_{\substack{j \geq k \\ \text{res}(\Gamma) = r}} \frac{1}{\text{sym}(\Gamma)} ; r \in R ; \quad (35)$$

be the sum of graphs with given residue $r \in R$ and loop number k . We have $\chi_r = 1 + \sum_{k=1}^{\infty} g^{2k} c_k^r ; r \in R_V$ and $\chi_r = 1 + \sum_{k=1}^{\infty} g^{2k} c_k^r ; r \in R_E$.

We call these formal sums χ^r combinatorial Green functions. Each term on their rhs maps under the Feynman rules to a contribution in the perturbative expansion of the Green functions of our gauge theory. Already the algebraic structure of these combinatorial Green functions is rather interesting. Analytic consequences will be briefly discussed at the end and explored in subsequent work.

Our task in this paper is to acquaint the reader with the structure of these sums, which is amazingly rich even at this elementary combinatorial level.

1.4 Insertion places

Each graph \mathcal{G} has internal edges $2^{[1]}_{\text{int}}$ and vertices $2^{[0]}$. We call (subsets of) those edges and vertices places of \mathcal{G} . Note that each place provides adjacent edges: for a vertex these are the edges attached to it, while each interior point of an edge defines two edges adjacent edges for it: the two pieces of the edge on both sides of that point. In such places, other graphs can be inserted, using a bijection between the external edges of those graphs and the adjacent edges provided by these very places.

The first thing we need to do is to count the number of insertion places with respect to the graphs to be inserted. Let $X = \bigsqcup_{i \in I} \mathcal{G}_i$ be a disjoint union of graphs to be inserted. Let us introduce variables a_r for all $r \in R$. To X we assign the monomial

$$x := \prod_{i \in I} a_{\text{res}(\mathcal{G}_i)} \quad (36)$$

This monomial defines integers $n_{X;s}$ for all $s \in R$ by setting

$$x = \prod_{s \in R} a_s^{n_{X;s}} \quad (37)$$

For example, if $X = \text{---}\bigcirc\text{---}\bigcirc\text{---}$, then

$$n_{X;\text{---}} = 2; n_{X;\bigcirc} = 0; s \notin \text{---} : \quad (38)$$

Furthermore, to a graph \mathcal{G} assign the function b , and integers $m_{;s}$ by

$$b := \prod_{v \in 2^{[0]}} a_v \prod_{e \in 2^{[1]}_{\text{int}}} \frac{1}{1 - a_e} = \prod_{s \in R_v} a_s^{m_{;s}} \prod_{e \in 2^{[1]}_{\text{ext}}} \frac{1}{[1 - a_e]^{m_{;e}}} \quad (39)$$

Then, we define the number of insertion places for X in \mathcal{G} , denoted \mathcal{K} , by

$$\mathcal{K} := \prod_{s \in R_v} \frac{m_{;s}}{n_{X;s}} \prod_{e \in 2^{[1]}_{\text{ext}}} \frac{a^{n_{X;e}} \frac{1}{[1 - a_e]^{m_{;e}}} (0)}{n_{X;e}!} \quad (40)$$

A few examples:

$$\text{---}\bigtriangleleft\text{---}\bigcirc\text{---} = 3; \text{---}\bigcirc\text{---}\bigcirc\text{---} = 2; \text{---}\bigcirc\text{---}\bigcirc\text{---}\bigcirc\text{---} = 1; \quad (41)$$

$$\text{---}\bigcirc\text{---}\bigcirc\text{---}\bigcirc\text{---} = 3; \quad (42)$$

as, for the last case,

$$a_{\text{---}}^2 \frac{1}{[1 - a_{\text{---}}]^2} (0) = 6: \quad (43)$$

1.5 Permutation of external edges

We call $j_{\mathcal{G}}$ the number of distinct graphs which are equal upon removal of the external edges. For example

$$\text{---}\bigcirc\text{---} = \text{---}\bigcirc\text{---} = \text{---}\bigcirc\text{---} = 3: \quad (44)$$

Such graphs can be obtained from each other by a permutation of external edges.

Furthermore for graphs $\mathcal{G}_1; \mathcal{G}_2$ we let $\text{top}(\mathcal{G}_1; \mathcal{G}_2)_p$ be the number of bijections between $2^{[1]}_{\text{ext}}$ and a chosen place $p = \text{res}(\mathcal{G}_2) \in 2^{[0]}_1 \cup 2^{[1]}_{\text{int}}$ such that \mathcal{G}_1 is obtained. This counts the number of ways to glue \mathcal{G}_2 into a chosen place $2^{[0]}_1$ to obtain \mathcal{G}_1 . This has a

straightforward generalization $\text{top}(\Gamma; X; \Gamma_p)$ to products of graphs X , where now p is an appropriate set of chosen residues $2 \begin{smallmatrix} [0] \\ 1 \end{smallmatrix} \begin{smallmatrix} [1] \\ 1; \text{int} \end{smallmatrix}$.

For example if $\Gamma = \text{loop}$, $\Gamma_1 = \text{loop}$, and p the vertex \times in Γ_1 , we have

$$\text{top}(\text{loop}; \text{loop}; \Gamma_p) = 2: \quad (45)$$

By definition, at a given place p ,

$$\text{top}(\Gamma; X; \Gamma_p) = \text{top}(\Gamma; \tilde{X}; \Gamma_p); \quad (46)$$

for all pairs $X; \tilde{X}$ related by a permutation of external legs.

1.6 Ramification in graphs

Above, we have counted the number of ways $\text{top}(\Gamma; X; \Gamma_p)$ how to glue graph(s) X into a chosen single place $p \begin{smallmatrix} [0] \\ 1 \end{smallmatrix} \begin{smallmatrix} [1] \\ 1; \text{int} \end{smallmatrix}$ so as to obtain a given graph Γ . Furthermore, there might be various different places $p_i \in 2 \begin{smallmatrix} [0] \\ 1 \end{smallmatrix} \begin{smallmatrix} [1] \\ 1; \text{int} \end{smallmatrix}$ which provide a bijection for X such that the same Γ is obtained.

Let $\text{bij}(\Gamma_1; \Gamma_2; \Gamma)$ be the number of bijections between $2 \begin{smallmatrix} [1] \\ 2; \text{ext} \end{smallmatrix}$ and adjacent edges of places $p \in \text{res}(\Gamma_2)$ in Γ_1 such that Γ is obtained.

A graph is described by vertices, edges and relations. For any bijection as above, we understand that the relations in Γ_2 , together with the relations in Γ_1 which remain after removal of a chosen place, and the relations provided by the bijection combine to the relations describing the graph Γ .

We let $\text{fbij}(\Gamma_1; \Gamma_2; \Gamma)$ be the set of all such bijections which allow to form Γ from Γ_1 and Γ_2 and write, for each $b \in \text{fbij}(\Gamma_1; \Gamma_2; \Gamma)$,

$$b = \Gamma_1 b_2: \quad (47)$$

We declare $\text{top}(\Gamma_1; \Gamma_2; \Gamma_p)$ to be the number of such bijections restricted to a place p in Γ_1 .

We have a factorization into the bijections at a given place p , and the distinct bijections which lead to the same result at that place:

$$\text{bij}(\Gamma_1; \Gamma_2; \Gamma) = \text{top}(\Gamma_1; \Gamma_2; \Gamma) \text{ram}(\Gamma_1; \Gamma_2; \Gamma): \quad (48)$$

Here, $\text{ram}(\Gamma_1; \Gamma_2; \Gamma)$ counts the numbers of different places $p \in 2 \begin{smallmatrix} [0] \\ 1 \end{smallmatrix} \begin{smallmatrix} [1] \\ 1; \text{int} \end{smallmatrix}$ which allow for bijections such that

$$\Gamma_1 b_2 = \Gamma: \quad (49)$$

Note that for any two such places $p; p'$ we find precisely $\text{top}(\Gamma_1; \Gamma_2; \Gamma)$ such bijections:

$$\text{top}(\Gamma_1; \Gamma_2; \Gamma) = \text{top}(\Gamma_1; \Gamma_2; \Gamma)_p = \text{top}(\Gamma_1; \Gamma_2; \Gamma)_{p'}: \quad (50)$$

One immediately confirms that this number is indeed independent of the place p as we can pair off the bijections at p with the bijections at p' for any places $p; p'$, so that the factorization (48) of $\text{bij}(\Gamma_1; \Gamma_2; \Gamma)$ is straightforward.

We call this integer $\text{ram}(\Gamma_1; \Gamma_2; \Gamma)$ the ramification index: it counts the degeneracy of inserting a graph at different places – if the ramification index is greater than one, the

same graph can be obtained from inserting a graph γ_2 into a graph γ_1 at different places. For example

$$\text{ram } \text{---} \bigcirc \text{---} ; \text{---} \triangleleft ; \text{---} \diamond \text{---} = 2; \text{ram } \text{---} \bigcirc \text{---} ; \text{---} \square \text{---} ; \text{---} \diamond \text{---} = 1: \quad (51)$$

The generalization replacing γ_2 by a product of graphs X is straightforward. The motivation of the name comes from a comparison with the situation in the study of number fields which will be given in future work.

1.7 pre-Lie structure of graphs

The pre-Lie product we will use is a sum over all bijections and places of graph insertions. Hence it gives the same result for the insertion of any two graphs related by permutation of their external legs. One could formulate the Hopf and Lie structure hence on graphs with amputated external legs, but we will stick with the usual physicists convention and work with Feynman graphs which have external edges.

We define $n(\gamma_1; X; \gamma_2)$ as the number of ways to shrink X to its residue (a set of one or more places) in γ_1 such that γ_2 remains.

We define a bilinear map

$$\gamma_1 \circ \gamma_2 = \sum_{j_1, j_2}^X \frac{n(\gamma_1; \gamma_2; j)}{j_1 j_2} : \quad (52)$$

This is a finite sum, as on the rhs only graphs can contribute such that

$$j_1 j_2 = j_1 j_2 + j_1 j_2 : \quad (53)$$

We divide by the number of permutations of external edges $j_1 j_2$ to eliminate the degeneracy in $n(\gamma_1; \gamma_2; j)$, a number which is insensitive to the orientation of edges of γ_2 . Note that for a permutation, we have $j_1 a = j_1 b$. Here, perm indicates equivalence upon permutation of external edges.

For example,

$$\text{---} \bigcirc \text{---} \triangleleft = 2 \text{---} \diamond \text{---} : \quad (54)$$

while

$$\text{---} \bigcirc \text{---} (\triangleleft + \triangleleft) = \text{---} \diamond \text{---} + \text{---} \diamond \text{---} + \text{---} \diamond \text{---} + \text{---} \diamond \text{---} : \quad (55)$$

Proposition 3 This map is pre-Lie:

$$(\gamma_1 \circ \gamma_2) \circ \gamma_3 = \gamma_1 \circ (\gamma_2 \circ \gamma_3) = (\gamma_1 \circ \gamma_3) \circ \gamma_2 = \gamma_1 \circ (\gamma_3 \circ \gamma_2) : \quad (56)$$

Note that the graphs on the rhs have all the same residue as γ_1 . The proof is analogous to the one in [6]. For a product of graphs X we define similarly

$$\gamma_1 \circ X = \sum_{j_1}^X \frac{n(\gamma_1; X; j)}{j_1} : \quad (57)$$

This is a straightforward generalization of this map, but certainly not a pre-Lie product in that generality.

1.8 The Lie algebra of graphs

We let L be the corresponding Lie algebra, obtained by antisymmetrizing the pre-Lie product:

$$[1; 2] = 2 \quad 1 \quad 1 \quad 2; \quad (58)$$

The bracket $[\cdot]$ fulfils a Jacobi identity and we hence get a graded Lie algebra. Note that the terms generated by the Lie bracket involve graphs of different residue.

1.9 The Hopf algebra of graphs

Let H be the corresponding Hopf algebra. Let us quickly describe how it is found. To L , we assign its universal enveloping algebra

$$U(L) = \sum_{j=0}^{\infty} T(L)^{(j)}; \quad (59)$$

where $T(L)^{(j)} = L^{\otimes j}$ is the j -fold tensorproduct of L . In $U(L)$ we identify

$$1 \quad 2 \quad 2 \quad 1 = [1; 2]; \quad (60)$$

as usual. We let

$$h[1; 2] = \begin{matrix} 0; & 1 & \leftarrow & 2 \\ 1; & 1 & = & 2 \end{matrix}; \quad (61)$$

Here we understand that entries on the lhs of $h[\cdot]$ belong to the Lie algebra, entries on the rhs to the Hopf algebra.

We compute the coproduct from this pairing requiring

$$h[1; 2]; (\cdot) = h \quad 1 \quad 2 \quad 2 \quad 1; (\cdot); \quad (62)$$

and find the usual composition into subgraphs and cographs

$$(\cdot) = 1 + 1 \quad + \quad \sum_X \quad = : \quad (63)$$

The antipode $S : H \rightarrow H$ is

$$S(\cdot) = \sum_X S(\cdot) = : \quad (64)$$

The counit ϵ annihilates the augmentation ideal as usual [6, 7].

Furthermore, we define j_{aug} to be the augmentation degree, defined via the projection P into the augmentation ideal. Furthermore, for future use we let $c_{k,s}^r$ be the sum of graphs with given residue r , loop number k and augmentation degree s . H_{lin} is the span of the linear generators of H .

With the Hopf algebra comes its character group, and with it three distinguished objects: the Feynman rules ϕ , the R operation

$$= m(S_R \quad P); \quad (65)$$

(which is a character with regard to the double structure of Rotax/Baxter algebras [5]) and counterterm R .

Note that the forgetfulness upon insertion wrt the external legs (46) forces us to work with a symmetric renormalization scheme

$$S_R(\cdot_1) = S_R(\cdot_2); \quad (66)$$

for consistency, for all pairs $\gamma_1; \gamma_2$ which agree by a permutation of external edges.

Indeed, $\delta_{\gamma_1 \gamma_2} = \text{perm}_{\gamma_1 \gamma_2}$,

$$0 = \gamma_1 \gamma_2 \quad (67)$$

$$= (\gamma_1 \gamma_2) \quad (68)$$

$$= S_R(\gamma_1 \gamma_2)(\gamma); \quad (69)$$

upon using (65) and as $(\gamma_1 \gamma_2) = 0$, and similarly for all cographs of γ_1 and γ_2 .

1.10 External structures

In later work it will be useful to disentangle Green functions wrt to their form-factor decomposition. This can be easily achieved by the appropriate use of external structures [6].

We hence extend graphs to pairs $(\gamma; \gamma')$ where γ labels the form factor and γ' with a forgetful rule

$$\sum_{\gamma_2} (\gamma_1; \gamma_2) (\gamma_2; \gamma_3) = \sum_{\gamma_2} \frac{n(\gamma_1; \gamma_2 \gamma_3)}{j_2} (\gamma; \gamma_3); \quad (70)$$

This allows to separate the form-factor decompositions as partitions of unity $1 = \sum_{\gamma_2} P_{\gamma_2}$ in computationally convenient ways for which we will use in future work. If we do not sum over γ_2 we can extend our notation to marked graphs as in [6].

2 The theorems

In this section we state the main result. It concerns the role played by the maps B_+^{kr} to be defined here: they provide the equations of motion, ensure locality, and lead us to the Slavnov-Taylor identities for the couplings.

We start by defining a map

$$B_+^{kr} = \sum_{\substack{j \neq k \\ j \text{ aug} = 1 \\ \text{res}(\gamma) = r}} \frac{1}{\text{sym}(\gamma)} B_+ \gamma; \quad (71)$$

where B_+ is a normalized generalization of the pre-Lie insertion into γ defined by requiring B_+^{kr} to be Hochschild closed. To achieve this, we need to count the maximal forests of a graph γ . It is the number of ways to shrink subdivergences to points such that the resulting cograph is primitive. To define it more formally, we use Sweedler's notation to write $(X) = X^{(0)} X^{(0)}$. If $X = \sum_{\gamma} \gamma$ is a Hopf algebra element with γ graphs we write

$$(X) = c(X^{(0)}; X^{(0)}) X^{(0)} X^{(0)}; \quad (72)$$

which defines scalars $c(X^{(0)}; X^{(0)})$. Here, $X^{(0)}$ and $X^{(0)}$ are graphs and the section coefficients of the Hopf algebra $c(X^{(0)}; X^{(0)})$ are explicitly spelled out.

We now set

$$\text{maxf}(\gamma) = \sum_{j \text{ aug} = 1} \sum_{\gamma} c(\gamma^{(0)}; \gamma^{(0)}) h_{\gamma}; \quad (73)$$

Note that this counts precisely the ways of shrinking subgraphs to points such that a primitive cograph remains, as it should, using the pairing between the Lie and Hopf algebra and summing over all Lie algebra generators indexed by primitive graphs γ .

The same number can by definition be obtained from the section coefficients of the pre-Lie algebra:

$$\max f(\gamma) = \sum_{j \text{ aug}=1}^X \sum_{j \neq j} n(\gamma; X; j); \quad (74)$$

as each maximal forest has a primitive cograph and some subdivergences X of loop number $j \neq j$.

We have defined the pre-Lie product so that

$$X = \sum_{2H_{lin}}^X \frac{n(\gamma; X; j)}{j!}; \quad (75)$$

Now we define

$$B_+(X) = \sum_{2H_{lin}}^X \frac{b_{ij}(\gamma; X; j)}{j!} \frac{1}{\max f(\gamma)} \frac{1}{[j!]}; \quad (76)$$

for all X in the augmentation ideal. Furthermore, $B_+(I) = 1$.

Taking into account the fact that the pre-Lie product is a sum over all labelled composition of graphs and the fact that we carefully divide out the number of possibilities to generate the same graph, we can apply the corresponding results for rooted trees [3]. One concludes in analogy to Theorem 2:

Theorem 4 (the Hochschild theorem)

$$r = 1 + \sum_{2M_r}^X \frac{1}{\text{sym}(\gamma)} = 1 + \sum_{k=1}^X g^k \sum_{\substack{j \neq k \\ j \text{ aug}=1 \\ \text{res}(\gamma)=r}}^X \frac{1}{\text{sym}(\gamma)} B_+(X); \quad (77)$$

where $X = \sum_{v \in V} \sum_{e \in E} \sum_{i \in I} 1 = e$.

For the next theorem, we have to define the Slavnov-Taylor identities for the coupling. Consider

$$X_{k;r} = r X_{\text{coupl}}^k; \quad (78)$$

We set

$$X_{\text{coupl}} = 1 + \sum_{k=1}^X g^{2k} c_k^{\text{coupl}}; \quad (79)$$

which determines the c_k^{coupl} as polynomials in the c_j^r from the definition of X_{coupl} below. The Slavnov-Taylor identities for the couplings can be written as

$$\frac{\text{diagram 1}}{\text{diagram 2}} = \frac{\text{diagram 3}}{\text{diagram 4}} = \frac{\text{diagram 5}}{\text{diagram 6}} = \frac{\text{diagram 7}}{\text{diagram 8}}; \quad (80)$$

which results in identities in every order in g^2 and leads to define indeed a single coupling X_{coupl} which can be defined in four equal ways, each one corresponding to an interaction monomial in the Lagrangian:

$$X_{\text{coupl}} = \frac{\text{diagram 1}}{\text{diagram 2}} = \frac{\text{diagram 3}}{\text{diagram 4}} = \frac{\text{diagram 5}}{[\text{diagram 6}]^{3=2}} = \frac{q \text{diagram 7}}{\text{diagram 8}}; \quad (81)$$

Note that we read this identities as describing the kernel of the counterterm: they hold under the evaluation of the indicated series of graphs by the corresponding character S_R .

The following theorem follows on imposing these identities as relations between Hopf algebra elements order by order in g^2 . On the other hand, if we assume the following theorem, we would derive the existence of the Slavnov-Taylor identities from the requirement of the existence of the grading sub Hopf algebra furnished by the elements c_k^r .

Theorem 5 (the gauge theory theorem)

$$i) \quad r \quad 1 + \sum_{2M_r}^X \frac{1}{\text{sym}(\cdot)} = 1 + \sum_{k=1}^X g^k B_+^{k,r}(X_{k,r}) \quad (82)$$

$$ii) \quad (B_+^{k,r}(X_{k,r})) = I \quad B_+^{k,r}(X_{k,r}) + (\text{id} \quad B_+^{k,r})(X_{k,r}): \quad (83)$$

$$iii) \quad (c_k^r) = \sum_{j=0}^{X^k} \text{Pol}_j^r(c) \quad c_k^r \quad j; \quad (84)$$

where $\text{Pol}_j^r(c)$ is a polynomial in the variables c_m^r of degree j , determined as the order j coefficient in the Taylor expansion of $r[X_{\text{coupl}}]^j$.

3 Two-loop Example

3.1 One-loop graphs

This section provides an instructive example. We consider our non-abelian gauge theory and first list its one-loop graphs, which provide by definition maps from $H^1 \rightarrow H^1_{\text{lin}}$.

The maps $B_+^{k,r}$, we claim, furnish the Hochschild one-cocycles and provide the Dyson-Schwinger equations, in accordance with the Hochschild and gauge theorems. We study this for the selfenergy of the gauge boson to two-loops. We want in particular exhibit the fact that each such two-loop graph is a sum of terms each lying in the image of such a map and want to understand the role of Hochschild cohomology.

We have for example

$$B_+^{1, \text{wavy}} = \frac{1}{2} B_+^{\text{circle}} + \frac{1}{2} B_+^{\text{loop}} + B_+^{\text{triangle}} + B_+^{\text{box}} : \quad (85)$$

To find the one-loop graphs we simply have to apply these maps to the unit of the Hopf algebra of graphs, which is trivial:

$$\begin{aligned} c_1^{\text{wavy}} &= B_+^{1, \text{wavy}}(I) = B_+^{\text{circle}}(I) + \frac{1}{2} B_+^{\text{loop}}(I) + \frac{1}{2} B_+^{\text{triangle}}(I) + B_+^{\text{box}}(I) \\ &= \text{circle} + \frac{1}{2} \text{circle} + \frac{1}{2} \text{loop} + \text{triangle} \end{aligned} \quad (86)$$

and similarly

$$c_1^{\text{gluon}} = B_+^{\text{gluon}}(I) = \text{gluon} \quad (87)$$

$$c_1^{\text{ghost}} = B_+^{\text{ghost}}(I) = \text{ghost} \quad (88)$$

$$\begin{aligned} c_1^{\text{fermion}} &= B_+^{\text{fermion}}(I) + B_+^{\text{fermion}}(I) + B_+^{\text{fermion}}(I) \\ &+ \frac{1}{2} B_+^{\text{fermion}}(I) + B_+^{\text{fermion}}(I) + B_+^{\text{fermion}}(I) \end{aligned} \quad \#$$

$$\begin{aligned}
& + B_+ \text{ (triangle with dashed lines) } (I) + B_+ \text{ (triangle with dashed lines) } (I) \\
& = \text{ (triangle with dashed lines) } + \text{ (triangle with dashed lines) } + \text{ (triangle with dashed lines) } + \frac{1}{2} \text{ (triangle with dashed lines and a loop) } \\
& + \text{ (triangle with dashed lines and a loop) } + \text{ (triangle with dashed lines and a loop) } + \text{ (triangle with dashed lines) } + \text{ (triangle with dashed lines) } \\
& \text{c}_1 \text{ (triangle with dashed lines and a cross) } = B_+ \text{ (square with dashed lines) } (I) + B_+ \text{ (square with dashed lines) } (I) + B_+ \text{ (square with dashed lines) } (I) + B_+ \text{ (square with dashed lines) } (I) \\
& + B_+ \text{ (square with dashed lines) } (I) + B_+ \text{ (square with dashed lines) } (I) + B_+ \text{ (square with dashed lines) } (I) + B_+ \text{ (square with dashed lines) } (I) \\
& + B_+ \text{ (square with dashed lines) } (I) + \frac{1}{2} B_+ \text{ (square with dashed lines and a loop) } (I) + B_+ \text{ (square with dashed lines and a loop) } (I) + B_+ \text{ (square with dashed lines and a loop) } (I) \\
& + B_+ \text{ (square with dashed lines) } (I) + B_+ \text{ (square with dashed lines) } (I) + B_+ \text{ (square with dashed lines) } (I) + B_+ \text{ (square with dashed lines) } (I) \\
& + B_+ \text{ (square with dashed lines) } (I) + B_+ \text{ (square with dashed lines) } (I) + B_+ \text{ (square with dashed lines) } (I) + B_+ \text{ (square with dashed lines) } (I) \\
& = \text{ (square with dashed lines) } + \text{ (square with dashed lines) } + \text{ (square with dashed lines) } + \text{ (square with dashed lines) } \\
& + \text{ (square with dashed lines) } + \text{ (square with dashed lines) } + \text{ (square with dashed lines) } + \text{ (square with dashed lines) } \\
& + \text{ (square with dashed lines) } + \frac{1}{2} \text{ (square with dashed lines and a loop) } + \text{ (square with dashed lines and a loop) } + \text{ (square with dashed lines and a loop) } \\
& + \text{ (square with dashed lines) } + \text{ (square with dashed lines) } + \text{ (square with dashed lines) } + \text{ (square with dashed lines) } \\
& + \text{ (square with dashed lines) } + \text{ (square with dashed lines) } + \text{ (square with dashed lines) } + \text{ (square with dashed lines) } \\
& + \text{ (square with dashed lines) } + \text{ (square with dashed lines) } + \text{ (square with dashed lines) } + \text{ (square with dashed lines) } :
\end{aligned} \tag{89}$$

3.2 Two-loop graphs

We now want to calculate

$$\begin{aligned}
\text{c}_2 \text{ (double line) } & = B_+ \text{ (triangle with dashed lines and a loop) } (2\text{c}_1 \text{ (triangle with dashed lines) } + 2\text{c}_1 \text{ (triangle with dashed lines) }) + \frac{1}{2} B_+ \text{ (triangle with dashed lines and a loop) } (2\text{c}_1 \text{ (triangle with dashed lines) } + 2\text{c}_1 \text{ (triangle with dashed lines) }) \\
& + \frac{1}{2} B_+ \text{ (triangle with dashed lines and a loop) } (\text{c}_1 \text{ (triangle with dashed lines and a cross) } + \text{c}_1 \text{ (triangle with dashed lines) }) + B_+ \text{ (triangle with dashed lines and a loop) } (2\text{c}_1 \text{ (triangle with dashed lines) } + 2\text{c}_1 \text{ (triangle with dashed lines) });
\end{aligned} \tag{91}$$

upon expanding

$$\text{X } \text{ (triangle with dashed lines and a loop) } = \text{ (triangle with dashed lines and a loop) }^2; \tag{92}$$

$$\text{X } \text{ (triangle with dashed lines and a loop) } = \text{ (triangle with dashed lines and a loop) }; \tag{93}$$

$$\text{X } \text{ (triangle with dashed lines and a loop) } = \text{ (triangle with dashed lines and a loop) }^2; \tag{94}$$

$$X \text{ --- } \bigcirc = \frac{1}{i_2} ; \quad (95)$$

to order g^2 .

Let us do this step by step. Adding up the contributions, we should find precisely the two-loop contributions to the gauge-boson selfenergy, and the coproduct

$$(c_2^{\text{---}}) = c_2^{\text{---}} \text{ I + I } c_2^{\text{---}} + 2c_1^{\text{coupl}} c_1^{\text{---}} : \quad (96)$$

The minus sign appears on the rhs due to our conventions in (34).

Insertions in $\frac{1}{2}B_+$

Below, we will give coefficients like $\frac{1}{2} \mathfrak{J} \mathfrak{P} \frac{1}{2} \frac{1}{2} \mathfrak{J} \mathfrak{J}$ in the next equation, where the first entry is the symmetry factor of the superscript of B_+ , the second entry the symmetry factor of the graphs in the argument X , the third entry the integer weight of that argument, the fourth entry the number of insertion places, the fifth entry the number of maximal forests of the graphs on the rhs, the sixth entry is $\text{top}(\text{---}; X; \text{---})$ and the seventh entry is $\text{ram}(\text{---}; X; \text{---})$.

We start

$$\begin{aligned} \frac{1}{2}B_+ \text{ --- } \bigcirc &= 2 \text{ --- } \triangleleft + 2 \text{ --- } \triangleright = \frac{1}{2} \mathfrak{J} \mathfrak{P} \frac{1}{2} \frac{1}{2} \mathfrak{J} \mathfrak{J} \\ &= \frac{1}{4} \text{ --- } \triangleleft + \text{ --- } \triangleright + \text{ --- } \triangleleft + \text{ --- } \triangleright \\ &= \frac{1}{2} \text{ --- } \triangleleft + \text{ --- } \triangleright ; \end{aligned} \quad (97)$$

where indeed the symmetry factor for $\text{---} \bigcirc$ is $1=2$, the symmetry factor for the graphs appearing as argument is 1, and they appear with weight two. We have two three-gluon vertices in $\text{---} \bigcirc$, and hence two insertion places. Each graph on the right has two maximal forests, and for each graph the inserted subgraph can be reduced in a unique way to obtain $\text{---} \bigcirc$, so the ramification index is one, and the topological weight is unity as well.



Similarly for ghosts

$$\begin{aligned} \frac{1}{2}B_+ \text{ --- } \bigcirc &= 2 \text{ --- } \triangleleft + 2 \text{ --- } \triangleright = \frac{1}{2} \mathfrak{J} \mathfrak{P} \frac{1}{2} \frac{1}{2} \mathfrak{J} \mathfrak{J} \\ &= \frac{1}{4} \text{ --- } \triangleleft + \text{ --- } \triangleright + \text{ --- } \triangleleft + \text{ --- } \triangleright \\ &= \frac{1}{2} \text{ --- } \triangleleft + \text{ --- } \triangleright : \end{aligned} \quad (98)$$



Next,

$$\begin{aligned} \frac{1}{2}B_+ \text{ --- } \bigcirc &= 2 \text{ --- } \triangleleft = \frac{1}{2} \mathfrak{J} \mathfrak{P} \frac{1}{2} \frac{1}{3} \mathfrak{J} \mathfrak{P} \text{ --- } \triangleleft \\ &= \frac{1}{3} \text{ --- } \triangleleft : \end{aligned} \quad (99)$$





$$\begin{aligned}
\frac{1}{2}\text{B}_+ &= \frac{1}{2} \left(\text{Diagram 1} + \text{Diagram 2} \right) \\
&= \frac{1}{2} \left(\text{Diagram 3} + \text{Diagram 4} \right) = \frac{1}{2} \left(\text{Diagram 5} + \text{Diagram 6} \right) :
\end{aligned}
\tag{103}$$
$$\begin{aligned}
\frac{1}{2} B_+ &= \frac{1}{2} \text{ (diagram with a loop on a horizontal line) } \\
&= \frac{1}{2} \frac{1}{2} \frac{1}{2} \frac{1}{2} \frac{1}{2} \frac{1}{2} \text{ (diagram with a loop on a horizontal line) } + \frac{1}{2} \text{ (diagram with a loop on a horizontal line) } \\
&= \frac{1}{8} \text{ (diagram with a loop on a horizontal line) } + \frac{1}{8} \text{ (diagram with a loop on a horizontal line) } \\
&= \frac{1}{4} \text{ (diagram with a loop on a horizontal line) } :
\end{aligned} \tag{104}$$

Insertions into $\frac{1}{2}B_+$ 
 We come to insertions into .



$$\begin{aligned}
\frac{1}{2} B_+ \quad & \text{[diagram: a horizontal line with a loop on top]} \\
& + \text{[diagram: a square with a vertical line through the center]} + \text{[diagram: a square with a vertical line through the center, rotated 90 degrees]} \\
& = \frac{1}{2} \text{[diagram: a horizontal line with a loop on top]} \frac{1}{3} \text{[diagram: a horizontal line with a loop on top]} \\
& + \frac{1}{2} \text{[diagram: a horizontal line with a loop on top]} \frac{1}{3} \text{[diagram: a horizontal line with a loop on top]} \\
& = \frac{1}{3} \text{[diagram: a horizontal line with a loop on top]} + \frac{1}{6} \text{[diagram: a horizontal line with a loop on top]} : \quad (105)
\end{aligned}$$

Indeed,  has three maximal forests, no ramification as there is only a single insertion place and two of the three bijections lead to it, while one bijection leads to , which also has three maximal forests.




$$\begin{aligned}
\frac{1}{2}B_+ &= \text{[diagram 1]} + \text{[diagram 2]} + \text{[diagram 3]} + \text{[diagram 4]} + \text{[diagram 5]} + \text{[diagram 6]} \\
&= \frac{1}{2} \text{[diagram 7]} \frac{1}{3} \text{[diagram 8]} + \frac{1}{2} \text{[diagram 9]} \frac{1}{2} \text{[diagram 10]} \\
&\quad + \frac{1}{2} \text{[diagram 11]} \frac{1}{3} \text{[diagram 12]} \text{[diagram 13]} + \text{[diagram 14]} + \text{[diagram 15]} \\
&= \frac{1}{6} \text{[diagram 16]} + \frac{1}{4} \text{[diagram 17]} + \frac{1}{3} \text{[diagram 18]} + \text{[diagram 19]} + \dots
\end{aligned}
\tag{106}$$

Note that  has three maximal forests and comes from one bijection,  has two maximal forests and comes as well from one bijection, while each of  and  come from two bijections and have three maximal forests.

$$\begin{aligned}
\frac{1}{2}B_+ \text{ (line with loop) } &= \frac{1}{2} \left(\text{X} + \text{X} + \text{X} \right) = \\
\frac{1}{2} \frac{1}{2} \text{ (line with loop) } &+ \frac{1}{2} \frac{1}{2} \frac{1}{3} \text{ (line with loop) } = \\
&= \frac{1}{8} \text{ (line with loop) } + \frac{1}{6} \text{ (line with loop) } : \quad (107)
\end{aligned}$$

This time,  has two maximal forests and comes from one bijection while  has three maximal forests and the two remaining bijections are leading to it.

$$\begin{aligned}
\frac{1}{2}B_+ \text{ (line with loop) } &= \frac{1}{2} \left(\text{X}_0 + \text{X}_1 + \text{X}_1 + \text{X}_1 + \text{X}_1 + \text{X}_1 \right) = \\
\frac{1}{2} \frac{1}{2} \text{ (line with loop) } &+ \frac{1}{2} \frac{1}{2} \frac{1}{3} \text{ (line with loop) } = \\
&= \frac{1}{2} \text{ (line with loop) } + \frac{1}{3} \text{ (line with loop) } : \quad (108)
\end{aligned}$$

Indeed,  and  have both two maximal forests and two bijections leading to them each, while  has three maximal forests and is generated from two bijections.

Similarly for ghosts

$$\begin{aligned}
\frac{1}{2}B_+ \text{ (line with loop) } &= \frac{1}{2} \left(\text{X}_0 + \text{X}_1 + \text{X}_1 + \text{X}_1 + \text{X}_1 + \text{X}_1 \right) = \\
\frac{1}{2} \frac{1}{2} \text{ (line with loop) } &+ \frac{1}{2} \frac{1}{2} \frac{1}{3} \text{ (line with loop) } = \\
&= \frac{1}{2} \text{ (line with loop) } + \frac{1}{3} \text{ (line with loop) } : \quad (109)
\end{aligned}$$

Now insertion of selfenergies.

$$\frac{1}{2}B_+ \text{ (line with loop) } = \frac{1}{2} \text{ (line with loop) } = \frac{1}{12} \text{ (line with loop) } ; \quad (110)$$

straightforward.

$$\frac{1}{2}B_+ \text{ (line with loop) } = \frac{1}{2} \text{ (line with loop) } = \frac{1}{8} \text{ (line with loop) } ; \quad (111)$$

ditto. Next,

$$\frac{1}{2}B_+ \text{ (with a loop) } - \text{ (with a bubble) } = \frac{1}{2} \text{ (with a chain of four bubbles) } - \text{ (with a chain of four bubbles and a loop) } = \frac{1}{2} \text{ (with a chain of four bubbles and a loop) } \quad (112)$$

and similar for the ghost-loop

$$\frac{1}{2} B_+ = \frac{1}{2} \text{(circle)} = \frac{1}{2} \text{(chain of 6 vertices)} = \frac{1}{2} \text{(triangle)} = \frac{1}{2} \text{(square)} : \quad (113)$$

This concludes insertions into $\underline{\Omega}$.

Insertions into B_+ and B_+
 It remains the insertions into B_+ and B_+ .

$$B_+ \quad 2 \quad = \quad 1 \frac{1}{2} \frac{1}{2} \frac{1}{3} \frac{1}{2} \quad = \frac{2}{3} \quad : \quad (114)$$

Indeed, there are three maximal forests, a ramification index of two and just a single bijection for each place.

N ext

$$\begin{aligned}
B_+ \quad \text{[diagram: a circle with two external lines]} &= 1 \, \text{[diagram: a vertex with two external lines]} \, \frac{1}{2} \, \text{[diagram: a vertex with two external lines]} \, \frac{1}{2} \, \text{[diagram: a vertex with two external lines]} \\
&= \frac{1}{2} \, \text{[diagram: a diamond with two external lines]} + \text{[diagram: a diamond with two external lines]} : \quad (115)
\end{aligned}$$

This time we have no ramification and two maximal forests.

Next the self-energy,

$$B_+ = \frac{1}{2} \left(\text{Diagram 1} + \text{Diagram 2} \right) = \frac{1}{2} \left(\text{Diagram 3} + \text{Diagram 4} \right) : \quad (116)$$

Again, two maximal forests, single bijection and no ramification.

Finally, the ghosts bring nothing new :

$$B_+ \quad \text{[diagram: a circle with a horizontal line through its center, with a dot on the line to the left of the circle and an arrow pointing right from the circle's center]} \quad 2 \quad \text{[diagram: a triangle with a horizontal line on the left, a vertical line on the right, and a diagonal line from top-left to bottom-right, with an arrow pointing down from the top vertex]} \quad) \quad = \quad 1 \text{[diagram: a vertical line with an arrow pointing down]} \text{[diagram: a vertical line with an arrow pointing down]} \frac{1}{2} \frac{1}{3} \text{[diagram: a vertical line with an arrow pointing down]} \text{[diagram: a vertical line with an arrow pointing down]} \quad \text{[diagram: a diamond shape with a horizontal line through its center, with an arrow pointing right from the center]} \quad = \quad \frac{2}{3} \quad \text{[diagram: a diamond shape with a horizontal line through its center, with an arrow pointing right from the center]} \quad : \quad (117)$$

And

$$\begin{aligned}
B_+ \quad \text{[diagram: a circle with a dashed line and an arrow, and a solid line with an arrow]} \quad 2 \quad \text{[diagram: a vertex with two outgoing lines, one solid and one dashed]} \quad) \quad = \quad 1 \text{[diagram: a vertex with two outgoing lines, one solid and one dashed]} \frac{1}{2} \text{[diagram: a vertex with two outgoing lines, one solid and one dashed]} \frac{1}{2} \text{[diagram: a vertex with two outgoing lines, one solid and one dashed]} \quad + \quad \text{[diagram: a diamond with two incoming and two outgoing lines, one solid and one dashed]} + \text{[diagram: a diamond with two incoming and two outgoing lines, one solid and one dashed]} \\
= \quad \frac{1}{2} \quad \text{[diagram: a diamond with two incoming and two outgoing lines, one solid and one dashed]} + \text{[diagram: a diamond with two incoming and two outgoing lines, one solid and one dashed]} : \quad (118)
\end{aligned}$$

Also,

$$\begin{aligned}
 B_+ \left(\text{diagram} \right) &= \frac{1}{2} \left(\text{diagram} \right) + \frac{1}{2} \left(\text{diagram} \right) + \frac{1}{2} \left(\text{diagram} \right) + \frac{1}{2} \left(\text{diagram} \right) \\
 &= \frac{1}{2} \left(\text{diagram} \right) + \frac{1}{2} \left(\text{diagram} \right) + \frac{1}{2} \left(\text{diagram} \right) + \frac{1}{2} \left(\text{diagram} \right) : \quad (119)
 \end{aligned}$$

3.3 Adding up

Now we indeed confirm that the results adds up to c_2 . Adding up, we indeed find

$$\begin{aligned}
 &\frac{1}{2} \left(\text{diagram} \right) + \frac{1}{2} \left(\text{diagram} \right) + \frac{1}{2} \left(\text{diagram} \right) + \frac{1}{2} \left(\text{diagram} \right) \quad \text{from (97) + (115)} \\
 &+ \frac{1}{2} \left(\text{diagram} \right) + \frac{1}{2} \left(\text{diagram} \right) + \frac{1}{2} \left(\text{diagram} \right) + \frac{1}{2} \left(\text{diagram} \right) \quad \text{from (98) + (118)} \\
 &+ \frac{1}{2} \left(\text{diagram} \right) + \frac{1}{2} \left(\text{diagram} \right) \quad \text{from (99) + (105)} \\
 &+ \frac{1}{4} \left(\text{diagram} \right) \quad \text{from (100)} \\
 &+ \frac{1}{2} \left(\text{diagram} \right) + \frac{1}{2} \left(\text{diagram} \right) \quad \text{from (100) + (106)} \\
 &+ \frac{1}{2} \left(\text{diagram} \right) \quad \text{from (101) + (105)} \\
 &+ \left(\text{diagram} \right) \quad \text{from (102)} \\
 &+ \left(\text{diagram} \right) \quad \text{from (103)} \\
 &+ \frac{1}{4} \left(\text{diagram} \right) \quad \text{from (106) + (110)} \\
 &+ \frac{1}{2} \left(\text{diagram} \right) \quad \text{from (104) + (106)} \\
 &+ \frac{1}{4} \left(\text{diagram} \right) \quad \text{from (107) + (111)} \\
 &+ \frac{1}{6} \left(\text{diagram} \right) \quad \text{from (107)} \\
 &+ \frac{1}{2} \left(\text{diagram} \right) + \frac{1}{2} \left(\text{diagram} \right) \quad \text{from (108) + (116)} \\
 &+ \frac{1}{2} \left(\text{diagram} \right) + \frac{1}{2} \left(\text{diagram} \right) \quad \text{from (109) + (119)} \\
 &+ \left(\text{diagram} \right) \quad \text{from (108) + (114)} \\
 &+ \left(\text{diagram} \right) \quad \text{from (109) + (117)}
 \end{aligned}$$

$$\begin{aligned}
& + \frac{1}{2} @ \begin{array}{c} 0 \\ \text{---} \end{array} \begin{array}{c} 1 \\ \text{---} \end{array} \text{A} \quad \text{from (112)} \\
& + \frac{1}{2} @ \begin{array}{c} 0 \\ \text{---} \end{array} \begin{array}{c} 1 \\ \text{---} \end{array} \text{A} : \quad \text{from (113)}
\end{aligned}$$

We indeed confirm that the result is

$$c_2 = \sum_{\substack{j \geq 2 \\ \text{res}(\text{---}) = \text{---}}} \frac{X}{\text{sym}(\text{---})}; \quad (120)$$

the sum over all graphs at the given loop order, divided by their symmetry factors. This confirms the Hochschild theorem.

Furthermore, we find that

$${}^0(c_2) = 2c_1 \begin{array}{c} \text{---} \\ \text{---} \end{array} + 2c_1 \begin{array}{c} \text{---} \\ \text{---} \end{array} \frac{1}{2} B_+ \begin{array}{c} \text{---} \\ \text{---} \end{array} \quad (\text{I}) \quad (121)$$

$$+ c_1 \begin{array}{c} \text{---} \\ \text{---} \end{array} + c_1 \begin{array}{c} \text{---} \\ \text{---} \end{array} \frac{1}{2} B_+ \begin{array}{c} \text{---} \\ \text{---} \end{array} \quad (\text{I}) \quad (122)$$

$$+ 2c_1 \begin{array}{c} \text{---} \\ \text{---} \end{array} + 2c_1 \begin{array}{c} \text{---} \\ \text{---} \end{array} B_+ \begin{array}{c} \text{---} \\ \text{---} \end{array} \quad (\text{I}) \quad (123)$$

$$+ 2c_1 \begin{array}{c} \text{---} \\ \text{---} \end{array} + 2c_1 \begin{array}{c} \text{---} \\ \text{---} \end{array} B_+ \begin{array}{c} \text{---} \\ \text{---} \end{array} \quad (\text{I}) : \quad (124)$$

We now impose the Slavnov-Taylor identity, which allows us to write the above as

$$[2c_1^{\text{coupl}} c_1 \begin{array}{c} \text{---} \\ \text{---} \end{array}] B_+^{1, \text{---}}; \quad (125)$$

by expanding (80) to order g^2 . Vice versa, if we require that the coproduct defines a sub Hopf algebra on the c_j^x , we reobtain the Slavnov-Taylor identities

$$2c_1 \begin{array}{c} \text{---} \\ \text{---} \end{array} + 2c_1 \begin{array}{c} \text{---} \\ \text{---} \end{array} = c_1 \begin{array}{c} \text{---} \\ \text{---} \end{array} + c_1 \begin{array}{c} \text{---} \\ \text{---} \end{array} = 2c_1 \begin{array}{c} \text{---} \\ \text{---} \end{array} + 2c_1 \begin{array}{c} \text{---} \\ \text{---} \end{array} = 2c_1 \begin{array}{c} \text{---} \\ \text{---} \end{array} + 2c_1 \begin{array}{c} \text{---} \\ \text{---} \end{array} : \quad (126)$$

Hence we recover the Slavnov-Taylor identities for the couplings from the above requirement. Summarizing, we indeed find

$${}^0(c_2) = \sum_i 2c_1^{\text{coupl}} c_1 \begin{array}{c} \text{---} \\ \text{---} \end{array} \begin{array}{c} \text{---} \\ \text{---} \end{array} : \quad (127)$$

Note that the above indeed implies

$$b B_+^{1, \text{---}} \begin{array}{c} \text{---} \\ \text{---} \end{array} [X_{\text{coupl}}]^2 = 0; \quad (128)$$

where

$$B_+^{1, \text{---}} = \frac{1}{2} B_+ \begin{array}{c} \text{---} \\ \text{---} \end{array} + \frac{1}{2} B_+ \begin{array}{c} \text{---} \\ \text{---} \end{array} + B_+ \begin{array}{c} \text{---} \\ \text{---} \end{array} + B_+ \begin{array}{c} \text{---} \\ \text{---} \end{array} : \quad (129)$$

3.4 Hochschild closedness

Finally, it is instructive to see how the Hochschild closedness comes about. Working out the coproduct on say the combination $\frac{1}{6}$  + $\frac{1}{4}$  = :U we find

$$\begin{aligned}
\langle U \rangle &= U \quad 1 + 1 \quad U + \frac{3}{6} \text{ (crossing)} \quad \text{ (loop)} \quad + \frac{1}{4} \text{ (crossing)} \quad \text{ (loop)} \\
&+ \frac{1}{4} \text{ (loop)} \quad \text{ (loop)} \quad (130)
\end{aligned}$$

On the other hand, looking at the definition of c_1^{\times} , we find a mixed term

$$\frac{1}{2} \text{ (diagram 1) } + \text{ (diagram 2) } + \text{ (diagram 3) } = \frac{1}{2} \text{ (diagram 4) } ; \quad (131)$$

and we now see why we insist on a symmetric renormalization point.

Furthermore, we con rm

$$\begin{array}{l}
z \text{---}^3 | \text{---} \{ \\
n \quad \text{el} ; \text{XX} ; \text{O} = \\
\\
z \text{---}^2 | \text{---} \{ z \text{---}^1 | \text{---} \{ z \text{---}^6 | \text{---} \{ \\
top \quad \text{el} ; \text{XX} ; \text{O} \quad ram \quad \text{el} ; \text{XX} ; \text{O} \quad sym \quad \text{O} \\
\hline
\qquad \qquad \qquad sym \quad \text{el} \quad sym \quad \text{XX} \\
\qquad \qquad \qquad | \text{---} \{ z \text{---} \} | \text{---} \{ z \text{---} \} \\
\qquad \qquad \qquad \quad \quad \quad 2 \qquad \quad \quad 2
\end{array}
\tag{132}$$

as it must by our definitions.

4 Discussion

We have exhibited the inner workings of Hochschild cohomology in the context of the Dyson-Schwinger equations of a generic non-abelian gauge theories. As a first combinatorial exercise we related the Slavnov-Taylor identities for the couplings to the very existence of a sub Hopf algebra which is based on the sum of all graphs at a given loop order. From [1] we know that the existence of this sub Hopf algebra is the first and crucial step towards non-perturbative solutions of such equations. Further steps in that direction are upcoming.

To prepare for this we finish the paper with a short discussion of some further properties of our set-up. This is largely meant as an outlook to upcoming results obtained by combining the Hopf algebra approach to perturbation theory with the structure of Dyson-Schwinger equations.

4.1 Locality and Finiteness

The first result concerns the proof of locality of counterterms and finiteness of renormalized Hopf algebra. The structure

$$r = 1 + \sum_k g^{2k} B_+^{kr} (r \chi_{\text{coupl}})^k \quad (133)$$

allows to prove locality of counterterms and finiteness of renormalized Green function via induction over the augmentation degree, involving nothing more than an elementary application of Weinberg's theorem to primitive graphs [7]. It unravels in that manner the source of equisingularity in the corresponding Riemann-Hilbert correspondences [8, 12]. For the DSE equations, this implies that we can define renormalized Feynman rules via the choice of a suitable boundary condition. This leads to an analytic study of the properties of the integral kernels of $(B_+^{k,r}(I))$ to be given in future work. Furthermore, the sub-Hopf algebra of generators c_k^r allows for recursions similar to the ones employed in [1], relating higher loop order amplitudes to products of lower loop order ones. The most crucial ingredient of the non-perturbative methods employed in that paper is now at our disposal for future work.

4.2 Expansions in the conformal anomaly

The form of the arguments $X_{r;k} = {}^rX_{\text{coupl}}^k$ allows for a systematic expansion in the coefficients of the β -function which relates the renormalization group to the lower central series of the Lie algebra L . Indeed, if the β -function vanishes X_{coupl} is mapped under the Feynman rules to a constant, and hence the resulting DSE become linear, by inspection. One immediately confirms that the resulting Hopf algebra structure is cocommutative, and the Lie algebra hence abelian [11, 3]. This should relate dilatations in quantum field theory to the representation theory of that lower central series. It will be interesting to compare the results here and more general in [13] with the ones in [15] from this viewpoint.

4.3 Central Extensions

The sub-Hopf algebras underlying the gauge theory theorem remain invariant upon addition of new primitive elements – beyond the one-loop level they obtain the form of a hierarchy of central extensions, which clearly deserves further study. Indeed, if we were to use only $B_+^{1,r}$ instead of the full series of Hochschild one cocycles we would still obtain the same sub-Hopf algebra. Thus, this sub-Hopf algebra and the structure of the DSEs is universal for a chosen QFT in the sense of [11, 3].

4.4 Radius of convergence

The above structure ensures that the Green functions come as a solution to a recursive equation which naturally provides one primitive generator in each degree. This has remarkable consequences for the radius of convergence when we express perturbation theory as a series in the coefficients c_k^r , upon utilizing properties of generating functions for recursive structures [9].

4.5 Motivic picture

The primitives themselves relate naturally to motivic theory [10]. Each primitive generator is transcendentially distinguished, with the one-loop iterated integral providing the rational seed of the game. The relation to algebraic geometry, motivic theory and mixed Hodge structures coming from QFT as they slowly emerge in [10, 11, 12] are an encouraging sign of the deep mathematical underpinnings of local interacting quantum fields.

Acknowledgments

It is a pleasure to thank Christoph Bergbauer, David Broadhurst, Kunusch Ebrahim iFard, Ivan Todorov and Karen Yeats for stimulating discussions.

References

- [1] D. J. Broadhurst and D. Kreimer, Exact solutions of Dyson-Schwinger equations for iterated one-loop integrals and propagator-coupling duality, Nucl. Phys. B 600 (2001) 403 [arXiv:hep-th/0012146].
- [2] A. Connes and D. Kreimer, Hopf algebras, renormalization and noncommutative geometry, Commun. Math. Phys. 199 (1998) 203 [arXiv:hep-th/9808042].
- [3] C. Bergbauer and D. Kreimer, Hopf algebras in renormalization theory: Locality and Dyson-Schwinger equations from Hochschild cohomology, arXiv:hep-th/0506190, to appear.
- [4] C. Bergbauer and D. Kreimer, The Hopf algebra of rooted trees in Epstein-Glaser renormalization, Annales Henri Poincaré 6 (2005) 343 [arXiv:hep-th/0403207].
- [5] K. Ebrahim iFard, L. Guo and D. Kreimer, Integrable renormalization. II: The general case, Annales Henri Poincaré 6 (2005) 369 [arXiv:hep-th/0403118].
- [6] A. Connes and D. Kreimer, Renormalization in quantum field theory and the Riemann-Hilbert problem. I: The Hopf algebra structure of graphs and the main theorem, Commun. Math. Phys. 210 (2000) 249 [arXiv:hep-th/9912092].
- [7] D. Kreimer, Structures in Feynman graphs: Hopf algebras and symmetries, Proc. Symp. Pure Math. 73 (2005) 43 [arXiv:hep-th/0202110].
- [8] A. Connes and M. Marcolli, From physics to number theory via noncommutative geometry. II: Renormalization, the Riemann-Hilbert correspondence, and motivic Galois theory, arXiv:hep-th/0411114.
- [9] Jason Bell, Stanley Burris, and Karen Yeats, Counting Trees: The Universal Law $t(n) = C^{-n} n^{3/2}$, (preprint), math.CO/0512432, to appear.
- [10] S. Bloch, H. Esnault, D. Kreimer, Motives associated to graph polynomials, arXiv:math-ag/0510011.
- [11] D. Kreimer, The residues of quantum field theory: Numbers we should know, arXiv:hep-th/0404090, to appear.
- [12] A. Connes and M. Marcolli, Quantum fields and motives, J. Geom. Phys. 56, 55 (2006) [arXiv:hep-th/0504085].
- [13] K. Ebrahim iFard and D. Kreimer, Hopf algebra approach to Feynman diagram calculations, J. Phys. A 38 (2005) R385 [arXiv:hep-th/0510202].
- [14] Z. Bern, L. J. Dixon and V. A. Smirnov, Iteration of planar amplitudes in maximally supersymmetric Yang-Mills theory at three loops and beyond, Phys. Rev. D 72 (2005) 085001 [arXiv:hep-th/0505205].
- [15] A. V. Belitsky, G. P. Korchemsky and D. Mueller, Integrability of two-loop dilatation operator in gauge theories, arXiv:hep-th/0509121.
- [16] J. Berges, S. Borsanyi, U. Reinosa and J. Serreau, Nonperturbative renormalization for 2PI effective action techniques, Annals Phys. 320 (2005) 344 [arXiv:hep-ph/0503240].